

NEW DATA AND A REVISED STRUCTURAL MODEL FOR FERRIHYDRITE

RICHARD A. EGGLETON¹ AND
ROBERT W. FITZPATRICK²

¹ Geology Department, Australian National University
GPO Box 4, Canberra, ACT 2601, Australia

² CSIRO, Division of Soils, Glen Osmond
South Australia 5064, Australia

Abstract—Synthetic 2-line and 6-line ferrihydrite samples prepared from ferric nitrate solutions have the bulk compositions $\text{Fe}_4(\text{O},\text{OH},\text{H}_2\text{O})_{12}$ and $\text{Fe}_{4.6}(\text{O},\text{OH},\text{H}_2\text{O})_{12}$, respectively. The composition depends on crystal size, which averages 20 Å for 2-line and 35 Å for 6-line ferrihydrite. X-ray absorption edge spectra indicate the presence of tetrahedral Fe^{3+} , a conclusion supported by heating experiments which show the development of maghemite after heating to 300°C in the presence of N_2 , followed by the formation of hematite at higher temperatures. These two reactions are recorded on differential thermal analysis traces by exotherms at 350° and 450°C. Transmission electron microscopy shows that 2-line ferrihydrite has no *Z*-axis regularity but does show hexagonal 2.54-Å lattice fringes. Six-line ferrihydrite forms faceted crystals having 9.4-Å *c*-parameter only detectable in dark field. In bright field, 2.54-Å lattice fringes indicate greater atomic regularity than in 2-line ferrihydrite. Analysis of the X-ray powder diffraction pattern of 6-line ferrihydrite suggests a structure based on double-hexagonal close-packed oxygens, containing 36% Fe in tetrahedral sites. Selective chemical dissolution, surface area measurements, and magnetic susceptibility are consistent with the recorded properties of ferrihydrite.

Key Words—Crystal structure, Ferrihydrite, Iron, Magnetic susceptibility, Surface area, Synthesis, Thermal analysis, Transmission electron microscopy, X-ray absorption edge spectra.

INTRODUCTION

Among the soluble iron fraction of soils and weathered rocks, and formed as precipitates from oxidized, iron-rich ground waters, is the mineral ferrihydrite, a poorly crystalline, hydrated ferric oxyhydroxide (previously referred to as “amorphous” iron oxide-hydroxide) (Chukhrov *et al.*, 1973; Schwertmann and Fischer, 1973; Carlson and Schwertmann, 1981). Ferrihydrite is one of the sources of iron for the formation of more crystalline iron minerals such as goethite, lepidocrocite, and hematite in the weathering environment, and a number of recent studies have examined the conditions of iron mineral crystallization from ferrihydrite (see review by Schwertmann, 1987).

Identity between ferrihydrite and precipitated ferric hydroxide was established by Chukhrov *et al.* (1973). Spiro and Saltman (1969) summarized the results of research on the nature of the high molecular weight polymers formed by the hydrolysis of ferric salts. At pH < 2, polymers grow in less than 1 hr and form 70-Å spherical particles of molecular weight 150,000. Polymers from ferric nitrate solution have the approximate formula $\text{Fe}_4\text{O}_3(\text{OH})_4(\text{NO}_3)_2(\text{H}_2\text{O})_{1.4}$, with most of the nitrate and water on the polymer surface. If the pH rises much above 2.5, ferric hydroxide precipitates, presumably by cross-linking of the polymers. Consequently, the structural properties of such polymers

should be a useful guide to the nature of precipitated ferric hydroxide.

Material similar to ferrihydrite comprises the cores of ferritin macromolecules (Harrison *et al.*, 1967), and many previous workers (see Webb, 1975) have equated ferritin cores with ferrihydrite. Crichton (1973) summarized the data on the iron core of horse-spleen ferritin; the Fe:O ratio is 5:12 and the cores are 70–75 Å in diameter and contain about 4300 Fe atoms.

Ferrihydrites yield a variety of X-ray powder diffraction patterns, which range from two very broad maxima at about 2.54 and 1.5 Å, indicating very poorly crystalline material, to that of less poorly crystalline ferrihydrite which shows six broad but distinct peaks between 2.56 and 1.48 Å. Consequently, ferrihydrites have come to be described as, for example, 2-line, 4-line, or 6-line ferrihydrite. In this paper previous work on the properties of ferrihydrite is first reviewed because conflicting results and structural conclusions are dispersed through the literature of chemistry, earth science, biology, and medicine. The results of X-ray powder diffraction (XRD), thermal analysis, transmission electron microscopy (TEM), surface area measurement, magnetic susceptibility, and X-ray absorption edge spectroscopy for synthetic 2-line and 6-line ferrihydrite are then reported and used to support a revised model for the structure of 6-line synthetic ferrihydrite.

REVIEW OF PREVIOUS WORK

Synthetic ferrihydrite has been prepared by neutralizing a ferric salt solution (e.g., Murphy *et al.*, 1976), by dialyzing a ferric nitrate solution with distilled water (Towe and Bradley, 1967), and by oxidizing a ferrous salt (Schwertmann and Taylor, 1972). Neutralizing a ferric salt generally produces 2-line ferrihydrite, whereas dialysis produces 6-line ferrihydrite.

Ferrihydrite is soluble in ammonium oxalate (pH 3). Schwertmann and Fischer (1973) proposed the use of this reagent for the selective dissolution and estimation of ferrihydrite in soils.

Van der Giessen (1966) proposed a cubic unit cell for 6-line ferrihydrite, but did not suggest a structure. Towe and Bradley (1967) suggested a hexagonal cell ($a = 5.08$, $c = 9.4$ Å) and a crystal structure based on that of hematite; this model is generally accepted as the structure of ferrihydrite, although some doubts were raised by Chukhrov *et al.* (1973). The Towe and Bradley model contains four planes of oxygen arranged in hexagonal closest packing. Iron is in octahedral coordination, but displaced from the center of the octahedron, as it is in hematite. Three octahedra are present per layer in the unit cell, and iron occupies only one octahedral site in three of the layers, but two in the fourth layer. This arrangement leads to the 9.4 -Å c -axis and to the observed composition of $\text{Fe}_5\text{O}_7\text{H}_9$. Towe and Bradley (1967) reported general agreement between calculated and observed XRD intensities, but gave no atomic coordinates. They found no evidence for structural OH and concluded that the nine hydrogens in the formula were all present as water. Russell (1979) has since shown that about half the hydrogen is present as OH; he suggested a formula $\text{Fe}_2\text{O}_3 \cdot 2\text{FeO}(\text{OH}) \cdot 2.5\text{H}_2\text{O}$. Massover and Cowley (1973) found TEM evidence for 9 -Å lattice fringes crossed by 4.4 -Å fringes in the cores of ferritin molecules, and regarded this as confirmation of the Towe and Bradley structure.

Simultaneously with the publication of the Towe and Bradley model, Harrison *et al.* (1967) presented a model for the ferric oxyhydroxide core of ferritin based on XRD evidence and a composition of $\text{FeO}(\text{OH})$. The Harrison *et al.* model has $a = 2.96$ Å, $c = 9.4$ Å, a cell similar to that of Towe and Bradley, but with a of Towe and Bradley = $\sqrt{3}a$ of Harrison *et al.* The structure they proposed is based on double hexagonal closest packing of oxygens (a stacking sequence ABAC), with iron distributed randomly among all the octahedral and tetrahedral sites of the close-packed array. Brady *et al.* (1968) reported a third model from radial distribution function analysis of ferrihydrite formed by hydrolysis of ferric nitrate. They concluded that all the iron was in tetrahedral coordination, with an Fe–O distance of 2.1 Å. By contrast, Gray (1971) used electronic absorption spectroscopy to rule out tetrahedrally

coordinated iron. Goncharov *et al.* (1978), in a detailed investigation of precipitate formation during the hydrolysis of ferric nitrate, concluded on spectroscopic evidence that tetrahedral and octahedral iron existed in the solutions. In particular, they recognized the presence of a polymer containing tetrahedral iron coexisting with an octahedral complex at pH 3–9. The absorption from the tetrahedrally coordinated iron decreased with time (12 weeks), whereas that from the octahedral complex was not time dependent.

Heald *et al.* (1979) used the extended X-ray absorption fine structure (EXAFS) technique to assess the coordination of iron in ferritin and in hydrolyzed Fe^{3+} polymers. They distinguished two varieties of polymer: a soluble, spherical polymer (type A) identical with that described by Spiro *et al.* (1966) and an insoluble polymer (type B). Their results indicate that the coordination number of iron in the soluble spherical polymer is 3.6, and in the insoluble polymer, 5.4. They concluded that iron in the soluble type A polymer is in distorted tetrahedral coordination and in distorted octahedral coordination in type B polymer and ferritin.

The magnetic properties of polynuclear iron proteins and various hydrolyzed Fe^{3+} polymers were extensively summarized by Webb (1975). Michaelis *et al.* (1943) determined the magnetic moment of ferritin (3.8 Bohr magnetons (B.M.)) and of ferric hydroxide precipitated from a variety of ferric salts. The magnetic moments found for the precipitates depended on their method of preparation and ranged from: 5.91 B.M. for ionic bonds (five unpaired electrons), 3.87 B.M. for three unpaired electrons and mixed ionic-covalent bonds, and 1.73 B.M. for entirely covalent bonds with one unpaired electron. Mulay and Selwood (1954) subsequently explained their low value of 3.8 B.M. found for ferric perchlorate solutions at pH 2 as a consequence of the presence of diamagnetic $\text{Fe}_2(\text{OH})_2(\text{H}_2\text{O})_8^{4+}$ dimers. Coey and Readman (1973) accepted this explanation in their study of a natural ferric hydroxide gel, for which they reported an effective magnetic moment at room temperature of 3.68 B.M. Mackenzie and Bowden (1983) and Prasad and Ghildyal (1975) reported large values for the magnetic susceptibilities for ferric hydroxide precipitate (equivalent to 6.6 and 7.1 B.M., respectively).

The Mössbauer spectra of natural ferrihydrite, precipitated ferric hydroxide, and the ferritin core are essentially identical (Crichton, 1973; Murad and Schwertmann, 1980). Room-temperature Mössbauer spectra of ferrihydrite show a paramagnetic doublet that can be well fitted by two Lorentzian doublets with isomer shifts 0.34, 0.35 mm/s and quadrupole splittings of 0.89 and 0.45 mm/s (Murad and Schwertmann, 1980). At 4 K, the spectrum is a sextet and can be acceptably fitted by three sextets having identical isomer shifts and slightly differing quadrupole splittings.

Murad and Schwertmann (1980) concluded that these results "should not be taken as proof for the existence of discretely different iron sites . . . but rather indicate continuous variation of parameters, and therefore of environments of the iron nuclei." They compared the room-temperature spectrum to that of finely divided hematite, and interpreted the two doublets that fit their observations as arising from internal well-ordered regions and external poorly ordered regions.

Many ferrihydrite samples have been imaged by TEM, and all show an aggregate of spheres, ranging from 30 to 70 Å in diameter. Murphy *et al.* (1976) showed that the hydrated ferric hydroxide polycations are spherical, having a diameter of about 30 Å. Towe and Bradley (1967) showed spherical aggregates formed by precipitation from ferric chloride and iron micelles within the ferritin macromolecule, both about 30–50 Å in diameter. Massover and Cowley (1973) similarly showed 50-Å spheres from horse-spleen ferritin. Natural ferrihydrites were also shown to be aggregates of 30–50-Å spheres (Schwertmann and Fischer, 1973; Henmi *et al.*, 1980; Carlson and Schwertmann, 1981).

Several techniques used to measure the surface area of ferrihydrite particles all give values greater than about 100 m²/g; most values range between 200 and 600 m²/g (Schwertmann and Fischer, 1973; Childs *et al.*, 1982; Karim, 1984). According to Carlson and Schwertmann (1981), poorly crystalline ferrihydrites have less accessible surface area than do more highly crystalline samples because of a greater degree of aggregation of 2-line ferrihydrite. They also reported that adsorption by ethylene glycol monoethylether gives higher specific surface areas than by the BET single point method using Ar as the adsorption gas. Despite the wide variation in measurements, all the results are consistent with the observed particle size (by TEM) of about 50 Å.

The published differential thermal analysis (DTA) data for ferrihydrites and so-called "amorphous" Fe-oxides are variable. Pure synthetic ferrihydrite generally gives a single sharp exothermic DTA peak between 300° and 350°C (Carlson and Schwertmann, 1981; Schwertmann, 1979; Chukhrov *et al.*, 1973). This exothermic peak has been ascribed to the transformation of ferrihydrite to hematite, however, Schwertmann (1987) suggests that it results from energy released on the recrystallization of hematite. Several workers (Towe and Bradley, 1967; Lewis and Schwertmann, 1980; Karim, 1984; Mackenzie and Meldau, 1959) have also recorded a double DTA exothermic peak for pure synthetic ferrihydrite. Although no satisfactory explanation was given for the double exotherm, Mackenzie and Meldau (1959) suggested that the lower-temperature exotherm may be related to the coalescence of the fine particles and the higher temperature exotherm to the crystallization of hematite. Si-containing synthetic ferrihydrite gives a much weaker and broader

DTA peak at about 700°C rather than 300°C (Carlson and Schwertmann, 1981; Herbillon and Tron Vinh An, 1969). Natural ferrihydrite heated in N₂ does not normally give an exothermic peak, a phenomenon which Carlson and Schwertmann (1981) attributed to the possible incorporation of Si into the ferrihydrite structure (formation of Si–O–Fe bonds). In contrast to the extent of published DTA data, little detailed information is available on the thermogravimetric behavior of ferrihydrite.

In summary, the composition of synthetic ferrihydrite is believed to be between Fe₂O₃·3H₂O and Fe₂O₃·2H₂O, with Fe₅O₁₂H, the most generally accepted ratio. The iron coordination is variously thought to be all tetrahedral, all octahedral, or mixed, and the iron distribution is thought to be random or semi-random. Structural models have been proposed having both hexagonal close-packed oxygens and double-hexagonal close-packed oxygens. The size of the crystals ranges from 30 to 70 Å.

MATERIALS AND METHODS

Synthesis

Six-line ferrihydrite was prepared by a modification of the method of Towe and Bradley (1967) as follows: 5 g of Fe(NO₃)₃·9H₂O was dissolved in 500 ml of deionized H₂O at 75°C with vigorous stirring and left for 13 min before rapid cooling in ice water. The solution was dialyzed for 3 weeks with daily replacement of deionized water. The precipitate was then centrifuge-washed three times with deionized water before being dried with acetone and ether.

Two-line ferrihydrite was prepared as follows: 100 ml of 0.375 M NaOH was added slowly with vigorous stirring to 500 ml of 0.025 M Fe(NO₃)₃·9H₂O solution; the resultant precipitate (pH 6.95) was allowed to stand for 15 min. After the precipitate was thoroughly centrifuge-washed with deionized water it was dried by heating overnight in an air oven at 60°C and then gently crushed.

Thermal analysis

Differential thermal analysis (DTA) and thermogravimetric analysis (TGA) were carried out simultaneously on samples using a Rigaku TG-DTA infrared heating apparatus (Thermoflex 8100 series). Heating was carried out at a rate of 10°C/min under flowing N₂ atmosphere. Weight loss was determined on 20-mg samples in Pt crucibles at temperatures ranging from ambient to 1050°C. A DTA sensitivity of 25 μV was achieved with Pt-Rh thermocouples, using Al₂O₃ as a reference. To study the various transformation products and the proportion of ferrihydrite remaining after heating, heated samples were prepared by interrupting the DTA experiments at different temperatures, corresponding to different positions on the DTA peaks.

Chemical analysis

Fifty milligrams of sample was dissolved in 10 M HCl to ascertain total Fe (Fe_T). Duplicate samples were extracted with 10 ml of NH₄-oxalate (pH 3) in the dark (Schwertmann, 1964) on an end-over-end shaker for 2 hr and then centrifuged (Fe_O). The extracts were analyzed for Fe by atomic absorption.

X-ray powder diffraction

XRD patterns were obtained from gently pressed specimens of random orientation using a Philips PW 1710 instrument

fitted with variable slit, a graphite reflected-beam monochromator, and $\text{CoK}\alpha$ radiation.

X-ray absorption edge spectroscopy

An X-ray absorption edge spectrum was obtained to give information about metal-oxygen coordination. Van Nordstrand (1960) reported spectra for a variety of Cr, Mn, and Co compounds and recognized a distinctive spectral type (type IV) for tetrahedrally coordinated Mn and Cr. The spectrum is characterized by a small absorption peak close to the absorption edge. To investigate the coordination of iron in ferrihydrite, spectra were collected for 6-line ferrihydrite and the following compounds containing tetrahedral and octahedral iron: FePO_4 (quartz form), maghemite, goethite, and hematite.

A Siemens Type-F X-ray diffractometer was converted to an absorption edge spectrometer by placing a Ge (111) crystal in the normal sample position and the iron-rich specimens behind the receiving slit as a powder on Mylar support film. Using an Mo target, operated at 20 kV and 30 mA, and 0.125° divergence and 0.05 mm receiving slits, the samples were scanned in 0.005° steps. More than 70,000 counts per step were collected. Resolution, estimated from the half-width of the $\text{FeK}\alpha$ emission line, was 25 eV or 0.002 \AA .

Electron microscopy

High-resolution TEM images were obtained using a JEOL 200CX electron microscope to examine the synthetic 2-line and 6-line ferrihydrite aggregates dispersed on holey carbon support film. Bright field images were obtained at a nominal magnification of 810,000 using an objective aperture which included diffracted beams out to 1.4 \AA . Following the technique described by Massover and Cowley (1973), dark-field images were recorded using an axial aperture equivalent to 2.5 \AA radius, with the direct beam tilted so as to be just excluded. In bright field, oriented crystals were selected by their greater contrast; dark field conditions clearly showed a $9\text{-}\text{\AA}$ (001) repeat, allowing identification of crystals oriented with their Z-axis perpendicular to the electron beam. Electron beam heating appeared to warp the crystal aggregates; hence, some initially bright crystals (in dark field) lost contrast, but could be tilted back into orientation.

Surface area

Specific surface areas were measured by the BET single-point method using N_2 as the adsorption gas. Surface areas were also measured by ethylene glycol-monoethylether (EGME) adsorption (Eltantawy and Arnold, 1974).

Magnetic susceptibility

Magnetic susceptibility was determined by the Gouy method using mercury(II) cobaltitetrathiocyanate, $\text{HgCo}(\text{CNS})_4$, as a calibration standard at 23°C .

RESULTS

Thermogravimetric and selective chemical dissolution analyses

Figure 1 shows the TGA curves for 6-line and 2-line ferrihydrites. Both samples gave a smooth and continuous weight loss, totaling 19.65% (average of three measurements) for the 6-line sample and 25% for the 2-line sample. At temperatures $<100^\circ\text{C}$, 6-line ferrihydrite lost 4.95% by weight, or one quarter of its total weight loss. Two-line ferrihydrite lost 6% by weight at temperatures $<100^\circ\text{C}$. Saleh and Jones (1984) found

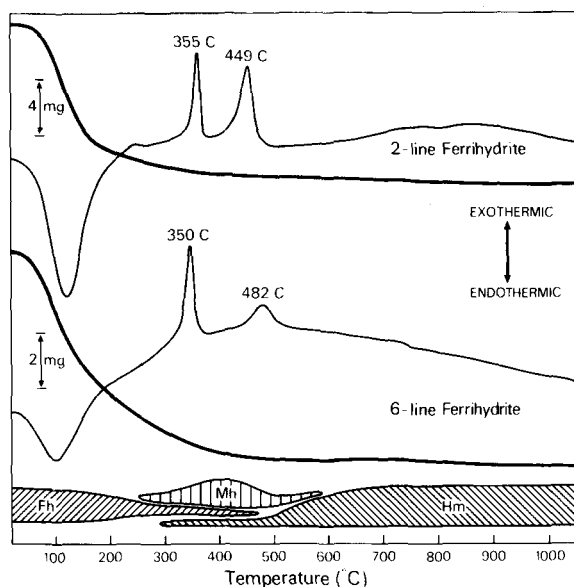


Figure 1. Differential thermal analysis curve (thin line), thermogravimetric curve (thick line), and mineral composition (diagrammatic; see also Figure 8) for 2-line and 6-line ferrihydrite. Fh = ferrihydrite, Mh = maghemite, Hm = hematite.

a weight loss of 22.4% for a synthetic 6-line ferrihydrite.

The two samples were almost completely soluble in NH_4 -oxalate as can be seen from the Fe_3/Fe_2 ratios (Table 1), results which conform with the data reported by Schwertmann and Fischer (1973) for synthetic and natural ferrihydrites, and which suggest the absence of other crystalline oxides or oxyhydroxides. These results indicate a composition (based on $12(\text{O} + \text{OH} + \text{H}_2\text{O})$) of $\text{Fe}_{4.63}\text{O}_{3.15}(\text{OH})_{7.59} \cdot 1.26\text{H}_2\text{O}$ for the 6-line ferrihydrite and $\text{Fe}_{4.03}\text{O}_{1.58}(\text{OH})_{9.0} \cdot 1.42\text{H}_2\text{O}$ for the 2-line ferrihydrite.

Surface area

BET- N_2 surface areas of 340 and $225 \text{ m}^2/\text{g}$ were found for 2-line and 6-line ferrihydrites, respectively. These results compare closely with those obtained by Saleh and Jones (1984) for 2-line ferrihydrite ($291 \text{ m}^2/\text{g}$) and by Karim (1984) for 6-line ferrihydrite ($249 \text{ m}^2/\text{g}$). The EGME surface areas for both the samples were about the same ($390 \pm 25 \text{ m}^2/\text{g}$). Carlson and Schwertmann (1981) also found that the EGME method gives a greater surface area than does the BET- N_2 method.

X-ray powder diffraction

The XRD traces from 20° to $90^\circ 2\theta$ reproduced in Figure 2 show that the samples as prepared conform to 2-line and 6-line ferrihydrite as described by Chukhrov *et al.* (1973), except for the presence of two broad peaks at about 4.5 and 3.25 \AA in the present patterns. The data to $145^\circ 2\theta$ ($d = 1 \text{ \AA}$) listed in Table 1 are similar to those of Towe and Bradley (1967).

Table 1. Properties of synthetic ferrihydrites.

	2-line ferrihydrite			6-line ferrihydrite		
X-ray powder diffraction:	<i>hk</i>	I	d (Å)	<i>hkl</i>	I	d (Å)
				002		4.5
				003		3.25
Intensities reported as peak heights.	11	100	2.5	110	100	2.52
Intensities for 6-line ferrihydrite after subtraction of 40% 2-line component.	30	55	1.5	112	77	2.23
				113	34	1.98
				114	33	1.72
				115	34	1.51
				300	76	1.46
				116	10	1.33
				220	12	1.27
				305	5	1.18
				225	12	1.07
Munsell color (Munsell, 1975)		5 YR 4/6			2.5 YR 4/6	
Weight loss (%):						
18°–100°C		6.0			4.95	
>100°C		19.0			14.7	
NH ₄ -oxalate extraction:						
Fe _o /Fe _t		1.0			0.95	
Specific surface area (m ² /g):						
BET-N ₂		340			225	
EGME		390 (±25)			390 (±25)	
Magnetic susceptibility:						
Mass susceptibility (e.m.u./g × 10 ⁻⁶)		130			113	
Molar susceptibility (e.m.u./mole × 10 ⁻⁶)		13,840			11,230	
Magnetic moment (B.M.)		5.75			5.17	
Crystal diameter (Å) (TEM measurement):						
Mean		20			35	
Range		15–30			20–55	
DTA exotherms (°C)		355			350	
		449			482	

Electron microscopy

Typical transmission electron micrographs of the 2-line and 6-line ferrihydrite samples are shown in Figures 3a and 3b, respectively. Both samples are highly aggregated, but the 6-line sample less so than the 2-line sample. The electron diffraction patterns of the ferrihydrite aggregates are similar to the XRD patterns and do not change after prolonged (10 min) electron-beam exposure. In bright-field conditions, the crystals appear to be agglomerated as rafts of crystals. Single crystals may project at the edges of the rafts, but commonly two or more crystals superimpose, introducing moiré fringes (see, e.g., Figure 5). The 6-line crystals range from 15 to 60 Å in diameter and are well faceted, showing the forms {001}, {112}, and {110}, indexed on the Towe and Bradley cell (Figures 4 and 5). Internally they have many defects (Figure 3b); hexagonal projections are the most perfect, although in some of

these the angle between lattice fringes deviates appreciably from 120°. Two-line crystals, being about 20–30 Å across, are smaller than 6-line crystals and show even less perfect {110} fringes.

In dark field, some 6-line crystals show a prominent 9.4-Å lattice repeat, separated by four 2.35-Å fringes. Bright field images of these crystals are variable, however, the clearest (Figures 4a and 5) show 2.5-Å lattice fringes perpendicular to a weak 9.4-Å structure. In some crystals the 9.4-Å regularity is interrupted by shorter (4.7 Å) or longer (13 Å) repeats (Figure 6). The crystals were quite stable under the electron beam, surviving for minutes with no apparent damage.

X-ray absorption edge spectroscopy

The X-ray absorption edge results for FePO₄ (tetrahedral Fe³⁺), maghemite (38% tetrahedral Fe³⁺), hematite and goethite (octahedral Fe³⁺), and the 6-line ferrihydrite are shown in Figure 7 (upper). The feature

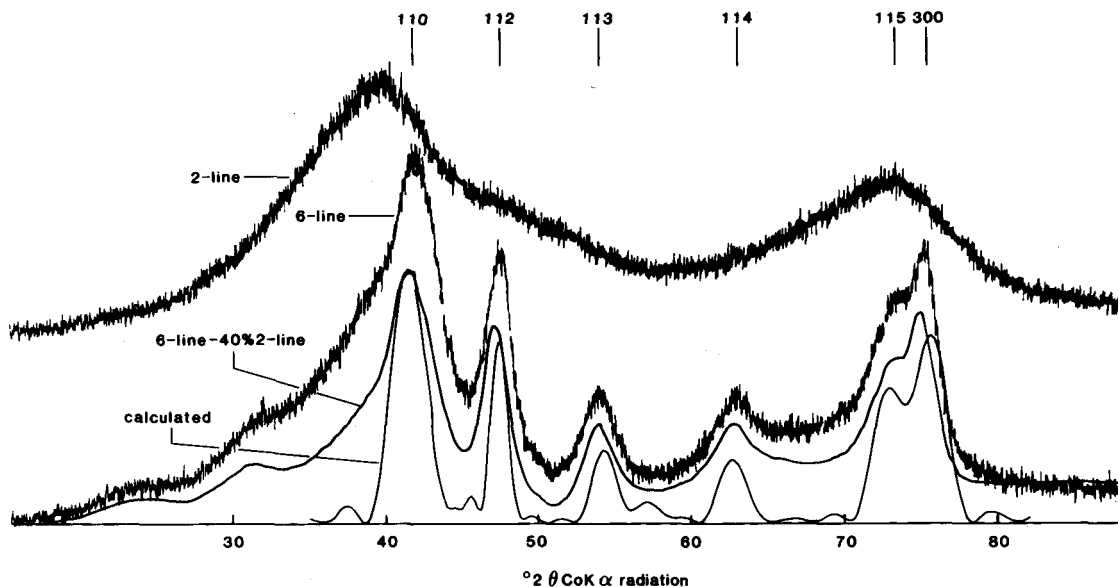


Figure 2. X-ray powder diffraction data: observed traces for 2-line and 6-line ferrihydrites, smoothed trace for 6-line with 40% 2-line ferrihydrite subtracted, and pattern calculated from parameters of Table 3, assuming 40-Å-size crystals.

thought to be indicative of tetrahedral Fe^{3+} is at 1.742 Å. The change of slope of the first derivative of the absorption spectrum in the vicinity of this feature is emphasized in Figure 7 (lower) for the above compounds, except botryoidal goethite which has a derivative spectrum very similar to that of hematite. These results indicate that the synthetic 6-line ferrihydrite contains about the same proportion of tetrahedral Fe^{3+} as the maghemite sample.

Differential thermal analysis

The combined TGA-DTA curves for the 2-line and 6-line ferrihydrites are illustrated in Figure 1. The DTA curves show a strong, sharp exothermic peak at about 340°–355°C followed by a broad exothermic peak at 449°C for the 2-line and 482°C for the 6-line samples. Compared to unheated ferrihydrite, the XRD patterns of the samples heated to 310°C show a sharpening of the 2.52-Å ferrihydrite peak and the introduction of three broad peaks at 3.7, 2.95, and 2.7 Å (Figure 8, curve b); the samples are ferrimagnetic. At 400°C (Figure 8c) the XRD pattern contains relatively sharp peaks of maghemite and hematite, whereas only hematite was detected in the patterns of the samples heated to 500°C. A summary of these results is included in Figure 1 based on XRD patterns from samples at room temperature, 310°C, and 400°C (Figure 8) plus similar results at 500°, 600°, and 1000°C.

Magnetic properties

The magnetic susceptibility values for both ferrihydrites are listed in Table 1; the values for the 6-line ferrihydrite are identical to those found by Van der

Giessen (1966) for an iron oxide gel prepared from ferric nitrate. The magnetic moment calculated from these results for 6-line ferrihydrite is 5.2 B.M./gram-atom Fe, and 5.7 B.M. for the 2-line ferrihydrite. These moments are within the range of 3.55–5.85 B.M. found by Michaelis *et al.* (1943) for colloidal ferric hydroxides, but larger than the value of 3.68 found by Coey and Readman (1973) for a natural ferric hydroxide gel.

INTERPRETATION OF RESULTS

Composition

To accommodate the inferred structural formula of $\text{Fe}_3(\text{O},\text{OH})_{12}$ in a 4-layer HCP cell, Towe and Bradley (1967) assumed that two Fe atoms per unit cell occupy the octahedral sites in one of the four layers, and that the other three layers held single Fe atoms. As outlined in the review of previous work, the composition of ferrihydrite appears to range widely on either side of this structural formula. An explanation for the variable Fe:O:H ratio may be found by considering the composition of very small crystals having an internal stoichiometry $\text{FeO}(\text{OH})$, with an (OH) surface. As can be seen from Table 2, a 75-Å crystal of $\text{FeO}(\text{OH})$ would have a composition close to $\text{Fe}_{5.0}(\text{O},\text{OH})_{12}$, whereas a 38-Å crystal would have a composition $\text{Fe}_{4.2}(\text{O},\text{OH})_{12}$. Russell (1979) observed that most of the H in ferrihydrite was easy to deuterate, the remainder more difficult, and he indicated an $\text{H}_2\text{O}:\text{OH}$ ratio of about 2.5:2. Small spheres 32 Å in diameter have a composition of about $(\text{FeO}(\text{OH}))_{3.9} \cdot 4.2\text{H}_2\text{O}$ with about two-thirds of the hydrogens on the surface of the sphere where they are presumably easier to deuterate than those in-

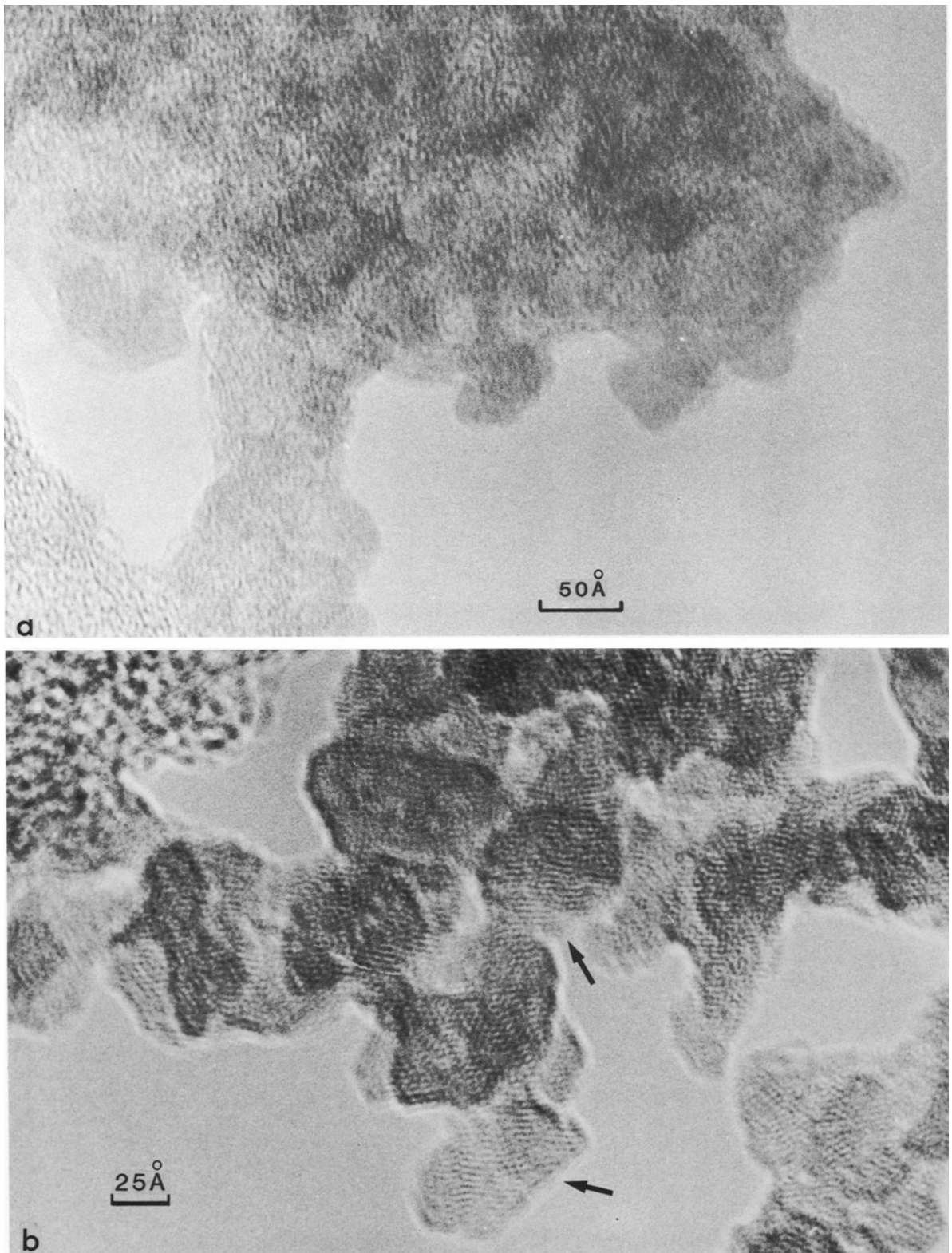


Figure 3. Transmission electron microscope images of ferrihydrite crystal aggregates: (a) 2-line ferrihydrite, (b) 6-line ferrihydrite. Irregularities in lattice rows are particularly obvious in the crystals arrowed.

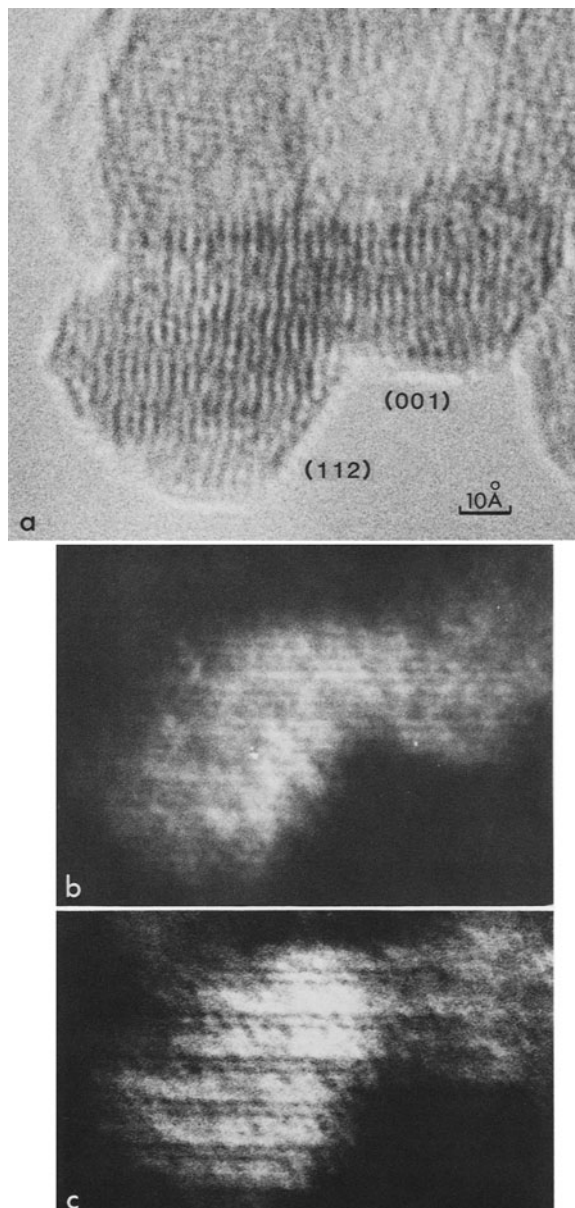


Figure 4. Transmission electron microscope images of 6-line ferrihydrite viewed parallel to $\langle 110 \rangle$. (a) Bright-field image showing (110) lattice fringes; (b), (c) dark-field images from the same crystal under different focus conditions, showing (b) 2.35-Å planes parallel to (001) and (c) contrast change every four layers.

side. Evidently a structural model for the unit cell need not conform to the bulk composition for such an aggregate of small crystals, and the ferrihydrite structure should be based on a structural formula of $\text{FeO}(\text{OH})$.

The change in composition with changing sphere size also influences other properties. The measured density for ferrihydrite ranges from 3.3 g/cm³, for natural samples (Childs *et al.*, 1982) to 3.96 g/cm³, for synthetic

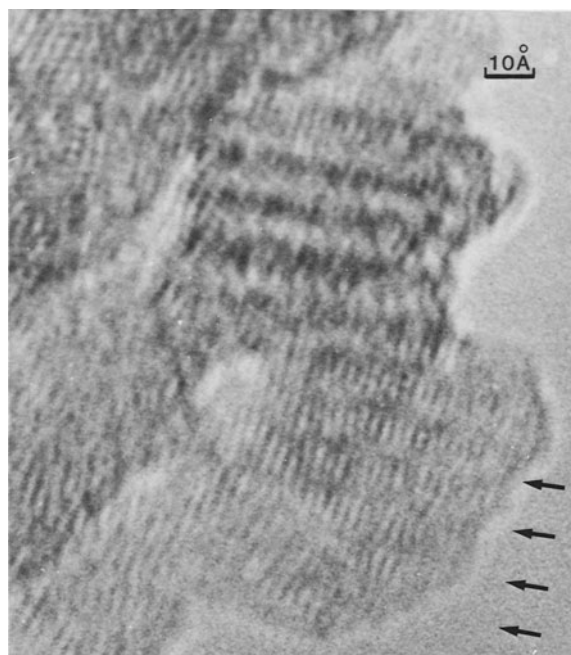


Figure 5. Transmission electron microscope images of partly overlapping ferrihydrite crystals with the same orientation (electron beam parallel to $\langle 1\bar{1}0 \rangle$). Upper crystal overlies a third, causing the prominent dark bands (moiré fringes).

material (Towe and Bradley, 1967). Calculated densities for small hexagonal crystals are listed in Table 2 and fall within the observed range.

X-ray powder diffraction

It is one of the properties of X-ray diffraction by crystals, that as crystal size decreases, peak widths increase, whereas the peak heights do not change at the Bragg position (see, e.g., Brindley, 1984). For this reason, peak intensities were measured as peak heights, not peak areas. Structure factors were obtained by correcting intensities for Lorentz and polarization factors and for multiplicity based on Towe and Bradley indexing. The 110 reflection from 2-line ferrihydrite is broad, peaking at 2.56 Å, which is at a slightly lower angle than the 110 peak from 6-line ferrihydrite (Figure 2). The 6-line pattern shows asymmetry on the low-angle side of the 110 reflection; this asymmetry is interpreted to result from the incorporation of some 2-line material in the sample. Subtraction of 40% of the intensity of the 2-line XRD pattern from the 6-line pattern removed most of the asymmetry, and the succeeding XRD structure analysis is based on corrected data (Figure 2, curve C). The broad peaks at about 4.5 and 3.25 Å were also reported by Towe and Bradley (1967) and are interpreted here as 002 and 003 reflections (Table 1).

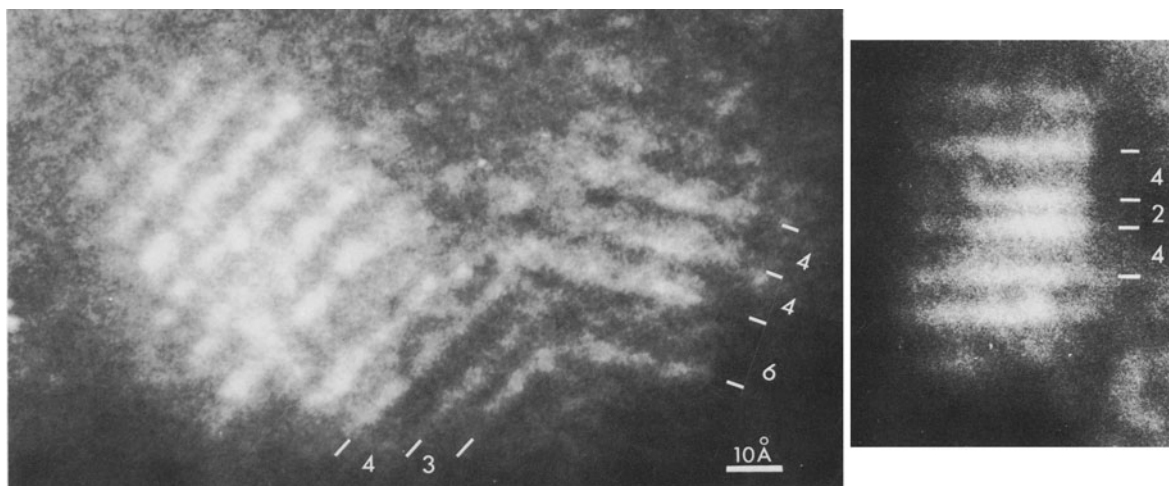


Figure 6. Three 6-line ferrihydrite crystals imaged in dark-field transmission electron microscope. Separation of the bright bands is interpreted in numbers of anion layers as 2, 3, 4, or 6.

Transmission electron microscopy

The high-resolution, bright-field images of 6-line ferrihydrite (Figures 4a and 5) show clear evidence for bands of high electron density perpendicular to (001), interpreted here as sheets of Fe-atoms parallel to (110). No evidence was found for planes of high electron density parallel to (001), nor for a more electron dense plane every 9.4 Å, as required by the Towe and Bradley structure. On the other hand, the dark field images of Figure 4 do show a 9.4-Å repeat of 2.35-Å fringes. Contrast in such images can arise from positional, rather than electron density variation, and thus could arise from changes in stacking sequence of either oxygen or iron. The imperfections evident in images of 6-line ferrihydrite *XY*-plane (Figure 3b) show that continuous lattice rows do not exist in these crystals; hence, detailed interpretation of the images is not possible. The results, however, are consistent with an oxygen stacking sequence ABAC as in the Harrison *et al.* model, with iron in columns 2.5 Å apart, as in the Towe and Bradley model, but having equal occupancy at all levels in the *Z*-direction.

Thermal analysis and surface area

The twin exotherms on the ferrihydrite DTA pattern and the XRD data for the heated samples (Figures 1

and 8) indicate a two-step reaction from ferrihydrite to the end-product hematite. The TGA curve shows that the first exotherm occurs just as the last 2% of water is lost from the sample. The presence of poorly crystalline maghemite at 310°C and of well-crystallized maghemite at 400°C suggests that the 350°C exotherm is largely the result of maghemite growth. The second exotherm is interpreted to result from the conversion of maghemite to hematite after dehydration is complete. The endotherm for 6-line ferrihydrite is broader and centered at lower temperature (105°C) than the endotherm for 2-line ferrihydrite (125°C). The relatively open nature of the 6-line sample (Figure 3) apparently allows water to be lost readily relative to that from the less-porous 2-line sample, leading to the lower temperature of the endothermic peak. The broader nature of the endotherm from 6-line ferrihydrite is attributed to the presence of some 2-line component (see X-ray powder diffraction section). The specific surface areas of ferrihydrite (Table 1) are much lower than the areas calculated from the observed crystal size (Table 2). Aggregation of the particles apparently prevented complete access by N₂ or EGME vapor to the entire crystal surface, leading to a low estimate of surface area (Carlson and Schwertmann, 1981), and retarded the escape of water during heating.

Table 2. Calculated composition, density, and specific surface area of truncated hexagonal bipyramidal crystals of ferrihydrite of various diameters.

Diameter (Å)	26	38	50	74	Large
Total (O + OH + H ₂ O)	361	1059	2327	7245	—
Total Fe	105	370	890	3031	—
Fe/12 anions	3.5	4.2	4.6	5.0	6.0
Density (g/cm ³)	3.2	3.5	3.6	3.8	4.3
Surface area (m ² /g)	1900	1200	860	550	—

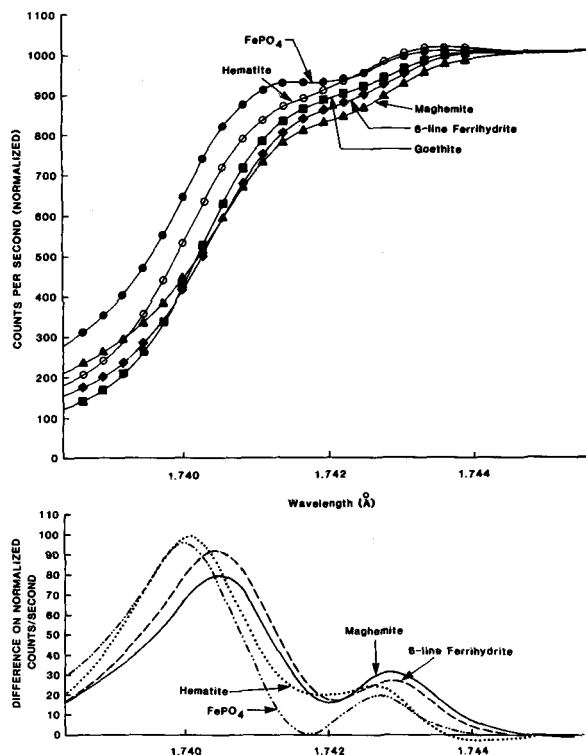


Figure 7. X-ray absorption spectra. (upper) For FePO_4 , maghemite, hematite, goethite, and 6-line ferrihydrate. Tetrahedral feature shows as a weak transmission drop between 1.742 and 1.743 Å. (lower) Derivative curves for the same phases, excluding goethite.

Magnetic properties

The magnetic moments determined here are close to those found for the aquo-ferric ion (5.92 B.M., Spiro and Saltman, 1969), but higher than those found for ferritin (3.8 B.M.) and $\text{Fe}_2\text{O}_3 \cdot 1.8\text{H}_2\text{O}$ (3.9 B.M., Webb, 1975) or a natural ferric gel (3.7 B.M., Coey and Readman, 1973). These differences suggest the absence of diamagnetic dimers in the two samples synthesized for this study (see "Review of previous work"). Thus, from the range of magnetic properties reported in the literature, the value of the susceptibility apparently depends on the mode of formation of ferrihydrate. Consequently, no structural interpretation can be made from these limited magnetic measurements.

PROPOSED STRUCTURE MODEL

Although the XRD d-spacing data do not favor the Towe and Bradley 5.08-Å *a*-axis over the Harrison *et al.* 2.96-Å *a*-axis, a description of the atomic arrangement requires the adoption of the larger unit cell. Both structure models suggest that disorder between layers leads to suppression of XRD reflections that suggest the 5.08-Å cell. Dark-field images for some examples show evidence for the larger *a*-axis.

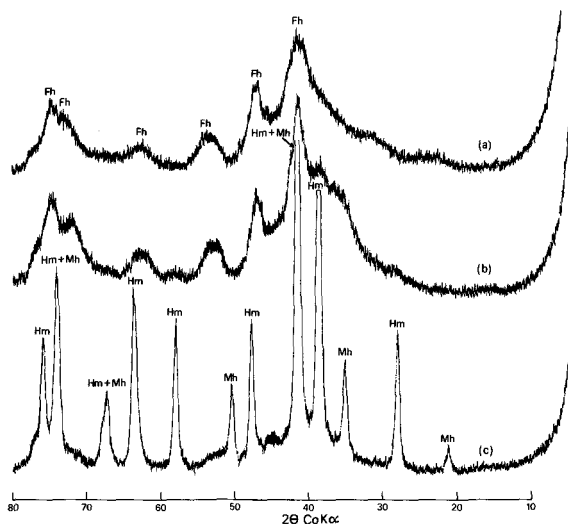


Figure 8. X-ray powder diffraction traces for 6-line ferrihydrate: (a) unheated, (b) heated to 310°C, (c) heated to 400°C.

Three independent experimental results point toward the presence of tetrahedral Fe^{3+} in ferrihydrate: (1) Goncharov *et al.* (1978) found spectroscopic evidence for tetrahedral iron in ferric solutions (see "Review of previous work"). (2) The X-ray absorption edge spectra reported here suggest a tetrahedral: octahedral iron ratio near that found in maghemite. (3) The first product of heating ferrihydrate was maghemite, a mineral having a spinel-type structure.

The model proposed here is based on double-hexagonal close packing of oxygens (ABAC), as in the Harrison *et al.* structure (Figure 9, upper). Two sheets of octahedrally coordinated iron are connected by two sheets of mixed tetrahedral and octahedral iron in the ratio 5 tetrahedral: 2 octahedral. This arrangement is similar to that in spinels and in so-called β -alumina (see, e.g., Clark, 1972). Along the 3-fold axes of spinel, planes of oxygens in cubic close packing alternately host all octahedral iron or mixed tetrahedral and octahedral iron. In β -alumina, four spinel-type sheets are connected by two sheets of tetrahedra sharing a common vertex, as is found also in $\text{KFe}_9\text{O}_{14}$ (Adelsköld, 1938).

The atomic coordinates listed in Table 3 were used to calculate XRD intensities. Some disorder in the iron positions was simulated by splitting the octahedral iron at $Z = 0, \frac{3}{4}$ into pairs of $\frac{1}{2}$ -atoms, 0.5 Å apart. The atoms were confined to ideal coordinates in double hexagonal close packing except that the *Z*-coordinate of the tetrahedral cations were adjusted to give best agreement between observed and calculated data. Total iron contents and overall temperature factor were also varied.

XRD structure factors for the trigonal, non-centrosymmetric model (space group $P31m$) are presented

Table 3. Atomic coordinates for 6-line ferrihydrite.

Atom	Coordination to oxygen	Towe and Bradley cell ¹			Fraction	Harrison <i>et al.</i> cell ²	
		X	Y	Z		X	Y
Fe 1a	octahedral	0	0	0.025	0.18	0	0
Fe 2b	octahedral	0	0	-0.025	0.18	0	0
Fe 2a	octahedral	0	0	0.725	0.18	0	0
Fe 2b	octahedral	0	0	0.775	0.18	0	0
Fe 3	tetrahedral	0	0	0.185	0.26	0	0
Fe 4	tetrahedral	0	0	0.565	0.26	0	0
Fe 5	octahedral	0	1/3	0.25	0.10	1/3	2/3
Fe 6	octahedral	0	1/3	0.50	0.10	1/3	2/3
OX1		1/3	1/3	1/8	1	2/3	1/3
OX2		0	0	3/8	1	0	0
OX3		1/3	1/3	3/8	1	2/3	1/3
OX4		0	1/3	7/8	1	1/3	2/3

¹ Towe and Bradley (1967) cell: $a = 5.08$, $c = 9.4$ Å, all coordinates $+(2/3, 1/3, 0)$; $+(1/3, 2/3, 0)$.

² Harrison *et al.* (1967) cell: $a = 2.96$, $c = 9.4$ Å. Space group $P3m1$, $Z = 1$; Formula $Fe_{1.44}O_4$.

in Table 4. The calculated and observed XRD patterns for the six strong lines are shown in Figure 2, curve d. In the intensity calculation used to prepare Figure 2, the structure factor term for continuously varying h and l was modulated by the diffraction function $\sin M\pi r \cdot s / \sin \pi r \cdot s$, where r is the relevant crystallographic direction and s is the reciprocal lattice vector. M , the number of unit cells in the direction r , was taken as 4 for (001) planes, 15 for the (110) planes and 26 for the (300) planes, so that $Md \approx 40$ Å. Instrumental line broadening was not included in the calculation.

The final atomic coordinates result from attempting to fit the X-ray diffraction intensities to a single structure; hence, they are unlikely to be a real description of ferrihydrite. Dark-field TEM images show that the dominant 4-layer sequence is interrupted by 3- or 6-layer sequences, which must also contribute to the XRD data and which therefore may explain the broad peaks interpreted as 002 and 003. Bright-field images show displacements of $[110]/3$ between some 4-layer packets, which will further modify the XRD intensities (see, e.g., Figure 5).

In the structure model shown in Figure 9 (lower), two octahedral sheets are followed by two dominantly tetrahedral sheets. The small amount of octahedral iron found at the level of the tetrahedra may represent stacking faults or changes in layer sequence and be caused by averaging. The total iron occupancy is equal at each level and conforms to the stoichiometry $Fe_6(O,OH)_{12}$ in a large crystal; however, the iron content is reduced to $Fe_{4.3}(O,OH)_{12}$ by the small crystal size and probably by omissions caused by structural defects.

The proposed model requires that the cations are randomly distributed over the available sites. In any layer, successive rings of polyhedra about the nucleation point are added as the crystal grows, with iron in

Table 4. Indices, d-values, observed $|Fo|$, and calculated $|Fc|$ X-ray diffraction structure factors for 6-line synthetic ferrihydrite.

hkl	d	$ Fo $	$ Fc $
002	4.7	15	24
003	3.13	32	9
110	2.52	52	55
111	2.47	— ¹	8
004	2.35	— ¹	21
112	2.23	38	38
113	1.98	29	28
005	1.88	<50 ²	33
114	1.72	34	30
115	1.51	50	51
300	1.46	87	89
116	1.33	27	29
220	1.27	28	32
305	1.18	18	19
225	1.07	27	30

¹ Obscured by 110.

² Based on profile height at $57^\circ 2\theta$ CoK α .

alternate polyhedra (Figure 10). If a site is occupied in one layer, it is vacant in the adjacent layers, except possibly for the two tetrahedral layers which may be linked apex to apex.

DISCUSSION

The proposed model has been derived largely from consideration of X-ray powder diffraction data, but the XRD results are too limited to allow further detail to be modeled. The XRD data do not agree with any model based on hexagonal close-packed oxygens and octahedral iron; they also rule out the Harrison *et al.* model which has equal and random occupancy of all octahedral and tetrahedral sites. The TEM lattice images, interpreted as showing dense planes of Fe-atoms parallel to (110) spaced at 2.54 Å, are in agreement with this new model.

The model presented here does not disagree with many earlier results which bear on the ferrihydrite structure and is supported by several other lines of evidence. The absorption edge spectrum presented here, although of low resolution, suggests a similar tetrahedral iron content to that of maghemite (37.5%), and the model, derived from XRD intensities, has 36% tetrahedral iron. The EXAFS results of Heald *et al.* (1979) for the insoluble ferric hydroxide polymer suggest a coordination number for Fe^{3+} of 5.4. A structure having 35% tetrahedral and 65% octahedral iron would have an average coordination number of 5.3. The combined TGA-DTA and XRD data that show the conversion of ferrihydrite to maghemite and hematite add considerable support to the presence of both tetrahedral and octahedral Fe in both 2-line and 6-line ferrihydrites. Goncharov *et al.* (1978) found positive spectroscopic evidence for tetrahedral and octahedral iron early in the hydrolysis of ferric nitrate.

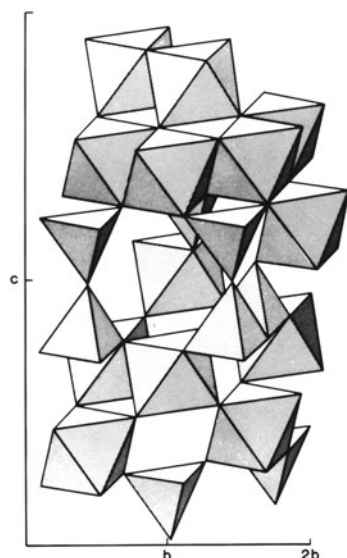
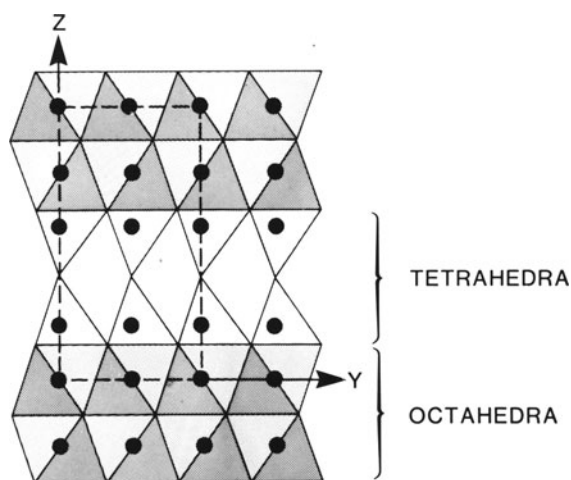


Figure 9. (upper) Model for 6-line ferrihydrite structure viewed along {110}. Coordinates of Table 3 include some octahedral iron at levels labeled "tetrahedral." All polyhedra are half-occupied, leading to an effective halving of the *b*-parameter. (lower) Clinographic drawing of linked polyhedra consistent with random occupancy of sites in the ferrihydrite model.

The XRD model composition $\text{Fe}_{4.3}(\text{O},\text{OH},\text{H}_2\text{O})_{12}$ has almost as much iron as found by direct analysis and is in agreement with the TEM results which show a crystal size range of 15–60 Å and imply a composition approximately $\text{Fe}_{4.2}(\text{O},\text{OH},\text{H}_2\text{O})_{12}$.

This study helps explain some of the questions posed by ferrihydrite. The broad XRD reflections probably result from small crystal size, not from deformed crystals or noncrystalline material. The random cation distribution may be responsible for the relative instability and small size of ferrihydrite crystals. Distortions re-

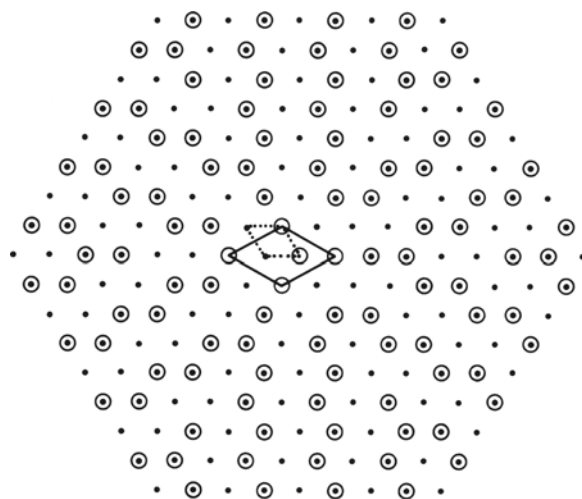


Figure 10. Possible pattern of polyhedron occupancy in any layer of ferrihydrite, caused by random filling of alternate sites on a concentric pattern. The Towe and Bradley (1967) unit cell is outlined solid, the Harrison *et al.* (1967) cell as a broken line.

sulting from a non-repeating pattern in each layer may restrict the extent of crystal growth. The role of silica in limiting ferrihydrite growth is probably a surface phenomenon, however, the presence of tetrahedral Si substituting for Fe^{3+} is possible according to the model and might introduce further distortions and limit growth. In addition, Carlson and Schwertmann (1981) showed that the exotherm temperature of synthetic and natural ferrihydrites can be influenced by Si content. They found a positive correlation between the percentage of Si coprecipitated with synthetic ferrihydrite and the thermal stability of the ferrihydrite. Si replacing Fe in tetrahedral sites might be expected to block the rearrangement in oxygen stacking required to form hematite (HCP) from a double HCP structure.

Most natural ferrihydrites contain appreciable silica, and synthetic ferrihydrites grown in siliceous solutions are generally the very poorly crystalline 2-line modification. Silica adsorbed on small ferrihydrite crystals may poison the surface and prevent further growth (Carlson and Schwertmann, 1981; Karim, 1984). If silica is adsorbed in the proportion of one Si to three surface oxygens, with an OH completing a surface tetrahedron, a 50-Å polycation would have a composition $\text{Fe}_{4.6}\text{Si}_{1.07}\text{O}_{6.08}(\text{OH})_{5.92}$. Childs *et al.* (1982) presented analyses of siliceous ferrihydrites whose particle size estimated from electron microscopy and surface area measurements was 50 Å. Recalculated to a total charge of 24+, the analyses of Childs *et al.* range from $\text{Fe}_{3.75}\text{Si}_{1.36}\text{O}_{4.64}(\text{OH})_{7.26}$ to $\text{Fe}_{5.1}\text{Si}_{0.9}\text{O}_7(\text{OH})_5$.

The double exotherm has been observed before by several workers (e.g., Towe and Bradley, 1967; Karim, 1984; Lewis and Schwertmann, 1980), but none have commented or given an explanation for it. The TGA-

DTA and magnetic evidence here has shown that the low-temperature exotherm can be attributed to the formation of an intermediate maghemite phase. The presence of tetrahedral and octahedral Fe in the ferrihydrite structure provides a plausible mechanism of formation. On the other hand, several published DTA studies on pure synthetic ferrihydrites have yielded single exotherms which are not consistent with our results, probably because the ferrihydrites were synthesized under different conditions. The synthesis results of Heald *et al.* (1979) show that two different polymers are readily produced during the hydrolysis of ferric salts, and Goncharov *et al.* (1978) concluded that the structure of the precipitate is determined by the structure of the polynuclear seeds, which in turn depend on the procedure used. Therefore, the crystal structure of ferrihydrite may be dependent on the mode of formation, and each study may be related to a somewhat different proportion of Fe in tetrahedral and octahedral coordination.

SUMMARY AND CONCLUSIONS

Synthetic 6-line ferrihydrite has the form of faceted 40–50-Å crystals. The stoichiometry is $\text{FeO}(\text{OH})$, modified by small crystal size and high surface water content to a composition of between $\text{Fe}_4(\text{OH})_{12}$ and $\text{Fe}_5\text{O}_3(\text{OH})_9$. The unit cell is trigonal, $a = 5.08 \text{ \AA}$, $c = 9.4 \text{ \AA}$, but a smaller cell, $a = 2.96 \text{ \AA}$, equally well describes the XRD data. The structure is based on double-hexagonal close-packed oxygens and hydroxyls, with two adjacent layers of iron in octahedral coordination followed by two layers of tetrahedral iron, probably sharing vertices. The iron distribution in any layer is semirandom giving an average iron occupancy of $\frac{1}{2}$ in each site, but with a tendency toward alternation between occupancy and vacancy for short distances, as revealed by dark-field electron microscopy. This more accurate definition of the structure of ferrihydrite permits correlations to be made between the crystal structure and its thermal transformation products and its ability to contain appreciable amounts of silica.

ACKNOWLEDGMENTS

The authors thank L. H. Smith and J. M. Thompson of the CSIRO Division of Soils for their respective assistance in surface area and thermal analysis determinations, and C. Foudoulis for the X-ray absorption edge measurements.

REFERENCES

- Adelsköld, V. (1938) X-ray studies on magneto-plumbite, $\text{PbO} \cdot 6\text{Fe}_2\text{O}_3$, and other substances resembling "beta-alumina", $\text{Na}_2\text{O} \cdot 11\text{Al}_2\text{O}_3$: *Arkiv för Kemi. Mineralogi Och Geologi* **12A**, 1–9.
- Brady, G. W., Kurkjian, C. R., Lyden, E. F. X., Robin, M. B., Saltman, P., Spiro, T., and Terzis, A. (1968) The structure of an iron core analog of ferritin: *Biochemistry* **7**, 2185–2192.
- Brindley, G. W. (1984) Order-disorder in clay mineral structures: in *Crystal Structures of Clay Minerals and their X-ray Identification*, G. W. Brindley and G. Brown, eds., Mineralogical Society, London, 495 pp.
- Carlson, L. and Schwertmann, U. (1981) Natural ferrihydrites in surface deposits from Finland and their association with silica: *Geochim. Cosmochim. Acta* **45**, 421–429.
- Childs, C. W., Downes, C. J., and Wells, N. (1982) Hydrous iron oxide minerals with short range order deposited in a spring/stream system, Tongariro National Park, New Zealand: *Aust. J. Soil Res.* **20**, 119–129.
- Chukhrov, F. W., Zvyagin, B. B., Ermilova, L. P., and Gorshov, A. I. (1973) New data on iron oxides in the weathering zone: in *Proc. Int. Clay Conf., Madrid, 1970*, J. M. Serratosa, ed., Div. de Ciencias, C.S.I.C., Madrid, 333–341.
- Clark, G. M. (1972) *The Structures of Non-molecular Solids*: Applied Science, London, 365 pp.
- Coe, J. M. D. and Readman, P. W. (1973) Characterization and magnetic properties of natural ferric gel: *Earth Planet. Sci. Letters* **21**, 45–51.
- Crichton, R. R. (1973) Ferritin: *Structure and Bonding* **17**, 67–134.
- Eltantawy, J. M. and Arnold, P. W. (1974) Ethylene glycol sorption by homoionic montmorillonites: *J. Soil Sci.* **25**, 99–110.
- Goncharov, G. N., Efimov, A. A., Kalyamin, A. V., and Tomilov, S. B. (1978) Mechanism of hydrolytic precipitate formation in the hydrolysis of Fe(III) in nitrate solutions: *Zh. Obshchei Khimii* **48**, 2398–2408 (in translation).
- Gray, H. B. (1971) Structural models for iron and copper proteins based on spectroscopic and magnetic properties: *Advan. Chem. Ser.* **100**, 365–389.
- Harrison, P. M., Fischbach, F. A., Hoy, T. G., and Haggis, G. M. (1967) Ferric oxyhydroxide core of ferritin: *Nature* **216**, 1188–1190.
- Heald, S. M., Stern, E. A., Bunker, B., Holt, E. M., and Holt S. L. (1979) Structure of the iron-containing core in ferritin by the extended X-ray absorption fine structure technique: *J. Amer. Chem. Soc.* **101**, 67–73.
- Henmi, T., Wells, N., Childs, C. W., and Parfitt, R. L. (1980) Poorly ordered iron-rich precipitates from springs and streams on andesitic volcanoes: *Geochim. Cosmochim. Acta* **44**, 365–372.
- Herbillon, A. J. and Tran Vinh An, J. (1969) Heterogeneity in silicon-iron mixed hydroxides: *J. Soil Sci.* **20**, 223–235.
- Karim, Z. (1984) Characteristics of ferrihydrites formed by oxidation of FeCl_2 solutions containing different amounts of silica: *Clays & Clay Minerals* **32**, 181–184.
- Lewis, D. G. and Schwertmann, U. (1980) The effect of (OH) on the goethite produced from ferrihydrite under alkaline conditions: *J. Colloid Interface Sci.* **78**, 543–553.
- Mackenzie, K. J. D. and Bowden, M. E. (1983) The effect of magnetic fields on the thermal decomposition reactions of inorganic hydroxy-compounds: *J. Mater. Sci. Lett.* **2**, 33–36.
- Mackenzie, R. C. and Meldau, R. (1959) The ageing of sesquioxide gels. I. Iron oxide gels: *Mineral. Mag.* **32**, 153–165.
- Massover, W. H. and Cowley, J. M. (1973) The ultrastructure of ferritin macromolecules. The lattice structure of the core crystallites: *Proc. Nat. Acad. Sci.* **70**, 3847–3851.
- Michaelis, L., Coryell, C. D., and Granick, S. (1943) Ferritin III. The magnetic properties of ferritin and some other colloidal ferric compounds: *J. Biol. Chem.* **149**, 463–480.
- Mulay, L. N. and Selwood, P. W. (1954) Hydrolysis of Fe^{3+} : Magnetic and spectrophotometric studies on ferric perchlorate solutions: *J. Amer. Chem. Soc.* **77**, 2693–2701.
- Munsell (1975) *Munsell Soil Color Charts*: Munsell Color Co. Inc., Baltimore, Maryland.

- Murad, E. and Schwertmann, U. (1980) The Mössbauer spectrum of ferrihydrite and its relations to those of other iron oxides: *Amer. Mineral.* **65**, 1044–1049.
- Murphy, P. J., Posner, A. M., and Quirk, J. P. (1976) Characterization of hydrolyzed ferric iron solutions. A comparison of the effects of various anions in solution: *J. Colloid Interface Sci.* **56**, 312–319.
- Prasad, B. and Ghildyal, B. P. (1975) Magnetic susceptibility of lateritic soils and clays: *Soil Science* **120**, 219–229.
- Russell, J. D. (1979) Infrared spectroscopy of ferrihydrite: Evidence for the presence of structural hydroxyl groups: *Clay Miner.* **14**, 109–114.
- Saleh, A. M. and Jones, A. A. (1984) The crystallinity and surface characteristics of synthetic ferrihydrite and its relationship to kaolinite surfaces: *Clay Miner.* **19**, 745–755.
- Schwertmann, U. (1964) Differenzierung der Eisenoxid des Bodens durch Extraktion mit Ammoniumoxalat-Lösung: *Z. Pfl. Ernähr. Düng. Bodenk.* **105**, 194–202.
- Schwertmann, U. (1979) The influence of aluminium on iron oxides: Five clay minerals as sources of aluminium: *Soil Sci.* **128**, 195–200.
- Schwertmann, U. (1987) Some properties of soil and synthetic iron oxides: in *Iron in Soils and Clay Minerals*, J. W. Stucki, B. A. Goodman, and U. Schwertmann, eds., D. Reidel, Dordrecht, 203–250.
- Schwertmann, U. and Fischer, W. R. (1973) Natural “amorphous” ferric hydroxide: *Geoderma* **10**, 237–247.
- Schwertmann, U. and Taylor, R. M. (1972) The transformation of lepidocrocite to goethite: *Clays & Clay Minerals* **20**, 151–158.
- Spiro, T. G., Allerton, S. E., Renner, J., Terzis, A., Bils, R., and Saltman, P. (1966) The hydrolytic polymerization of iron(III): *J. Amer. Chem. Soc.* **88**, 2721–2726.
- Spiro, T. G. and Saltman, P. (1969) Polynuclear complexes of iron and their biological implications: *Structure and Bonding* **6**, 116–152.
- Towe, K. M. and Bradley, W. F. (1967) Mineralogical constitution of colloidal “hydrous ferric oxides”: *J. Colloid Interface Sci.* **24**, 384–392.
- Van der Giessen, A. A. (1966) The structure of iron(III) oxide-hydrate gels: *J. Inorg. Nucl. Chem.* **28**, 2155–2159.
- Van Nordstrand, R. A. (1960) X-ray absorption edge spectroscopy of compounds of chromium, manganese, and cobalt in crystalline and non-crystalline systems: in *Proc. Conf. Non-crystalline Solids*, V. D. Frechette, ed., Wiley, New York, 536 pp.
- Webb, J. (1975) Polynuclear iron(III) proteins: in *Techniques and Topics in Bioinorganic Chemistry*, C. A. McAuliffe, ed., Macmillan, London, 270–304.

(Received 11 December 1986; accepted 27 July 1987; Ms. 1628)